fine simple stain MAX-PO for 30 min at room temperature. Sections were washed and further incubated with the 3-amino-9-ethylcarbazole substrate-chromogen system (Nichirei Bioscience Inc.) for 10 min at room temperature. As negative controls, each isotype nonimmune serum (2 μg/mL) of the same species was used instead of the primary antibody. The sections were counterstained with Mayer's hematoxylin, mounted in Aquatex (Merck KGaA, Darmstadt, Germany) and examined with a BH2 light microscope (Olympus, Tokyo, Japan).

Immunofluorescence

To investigate the origin of high-mobility-group box 1 in the periodontitis tissues, paraffin-embedded sections (5 μm) of gingival tissues were deparaffinized in xylene and rehydrated through a series of decreasing concentrations of ethanol. After three washes with phosphate-buffered saline, the sections were blocked with 1% bovine serum albumin in phosphate-buffered saline for 1 h and then incubated with a rabbit anti-high-mobility-group box 1 polyclonal immunoglobulin (1 μg/mL) and human macrophage marker immunoglobulin (anti-CD68) for 1 h at room temperature. The sections were then washed with phosphate-buffered saline and incubated with fluorescein isothiocyanate-conjugated antirabbit IgG and rhodamine-conjugated antimouse IgG (Immunotech, Marseille, France), diluted 1 : 50 in phosphate-buffered saline, for 30 min at room temperature. Finally, cell nuclei were labeled with 4′,6-diamidino-2-phenylindole (Nakalai Tesque, Kyoto, Japan) and the sections were washed and examined using an Axioskop microscope (Carl Zeiss, Oberkochen, Germany).

Cell culture

Rat gingival epithelial cells were established from 2-wk-old Rowett rats and palatal gingival explants were prepared as described previously (22). Briefly, the palatal gingival explants were placed in tissue culture plates in Dulbecco's modified Eagle's medium (Sigma-Aldrich) containing 10% fetal bovine serum. After 2 wk, rat gingival epithelial cells were further cultured in keratinocyte serum-free medium (Life Technologies, Rockville, MD, USA) supplemented with epidermal growth factor (5 ng/mL) and bovine pituitary extract (30–50 μg/mL). The cells were used for the following experiments after four to six passages. A human gingival epithelial cell line (Ca9-22) was obtained from the Japanese Collection of Research Bioresources (JCRB, Osaka, Japan) and suspended in Eagle's minimal essential medium (Sigma-Aldrich), supplemented with 10% fetal bovine serum, at 37°C in a humidified 5% CO_2 atmosphere.

Sample preparation for western blot analysis

All samples were prepared as described previously (8), with slight modifications. Briefly, cells (8×10^5 cells/well) were stimulated, for 0–20 h, with tumor necrosis factor-α at 0, 1, 5 or 10 ng/mL in Eagle's minimal essential medium containing 1% fetal bovine serum. High-mobility-group box 1-containing supernatants (1 mL), in the presence or absence of tumor necrosis factor-α, were collected and further incubated overnight with 50 μL of heparin–Sepharose 6B (GE Healthcare Bio-Sciences AB, Uppsala, Sweden). After three washes with phosphate-buffered saline, sodium dodecyl sulfate sample buffer was added. For MAPK assays, the cells were lysed, as previously described (23). Briefly, 120-μL aliquots of cell suspensions (5×10^5 cells/dish) were seeded into 60-mm cell culture dishes, and cell lysates were obtained by adding 120 μL of sodium dodecyl sulfate sample buffer containing 50 mM dithiothreitol, 1 mM phenylmethanesulfonyl fluoride and 0.5 mM Na_2VO_3. The supernatants and lysates were assayed for their protein concentrations using a Protein Assay Kit (Bio-Rad, Hercules, CA, USA) and subjected to 12% sodium dodecyl sulfate-polyacrylamide gel electrophoresis. All experiments using inhibitors were performed as described above, except that the cells were preincubated with a tumor necrosis factor receptor 1-neutralizing antibody or respective MAPK inhibitors for 1 h before exposure to tumor necrosis factor-α.

Western blot analysis

After subjecting all the samples to 12% sodium dodecyl sulfate-polyacrylamide gel electrophoresis, the separated proteins were transferred to nitrocellulose membranes (Schleicher & Schuell, Dassel, Germany). The membranes were blocked with 5% nonfat dry milk in Tris-buffered saline (pH 7.4), containing 0.02% Tween 20, for 1 h at room temperature and then incubated with a primary antibody (anti-high-mobility-group box 1 immunoglobulin at 10 μg/mL or anti-MAPK immunoglobulins diluted 1 : 3000) in Tris-buffered saline (pH 7.4) containing 0.02% Tween 20 and 1% nonfat dry milk, overnight at 4°C. After three washes with Tris-buffered saline (pH 7.4) containing 0.02% Tween 20, the membranes were incubated with horseradish peroxidase-conjugated antirabbit IgG (Santa Cruz Biotechnology, Santa Cruz, CA, USA), diluted 1 : 3000 in Tris-buffered saline (pH 7.4) containing 0.02% Tween 20 and 2.5% nonfat dry milk, for 1 h at room temperature. Finally, the membranes were washed with Tris-buffered saline (pH 7.4) containing 0.02% Tween 20, and developed with an enhanced chemiluminescence kit (Amersham Pharmacia Biosciences, Bucks., UK).

Cell viability assay

The cell viabilities were analyzed by the mitochondrial respiratory activity, which was measured using the 3-(4,5-dimethylthiazol-2yl)-2,5-diphenol tetrazolium bromide (MTT) cleavage assay (Boehringer Mannheim, Indianapolis, IN, USA). This assay was performed using a slight modification of the method described by Twentyman *et al.* (24). Briefly, cells cultured in 96-well plates (with 100 μL of medium per well) were incubated with MTT (20 μL of 2.5 μg/mL per well) at 37°C for 3 h. The formazan product was solubilized by the addition of 100 μL of dimethylsulfoxide and 100 μL of 10% sodium

dodecyl sulfate (in 0.01 M HCl) for 16 h at 37°C. The dehydrogenase activity was expressed as the absorbance (read with an Immuno Mini NJ-2300 (Inter Medical, Tokyo, Japan)) at a test wavelength of 570 nm and a reference wavelength of 630 nm.

Statistical analysis

Inhibition of individual MAPKs study and cell viability test were calculated from three separate experiments and expressed as the mean ± standard deviation. The Bonferroni correction was used for multiple *t*-test comparisons, and *p*-values were determined using STATVIEW version 5.0 for Macintosh. Values of $p < 0.05$ were considered statistically significant.

Results

High-mobility-group box 1 expression in human inflamed gingival crevicular fluid and chronic periodontitis tissues

Gingival crevicular fluid contains a rich array of biochemical factors that reflect the metabolic status of the periodontal tissue component (25). By western blot analysis, high-mobility-group box 1 was detected in the gingival crevicular fluid from periodontitis subjects, but not in that from control subjects (Fig. 1). To explore high-mobility-group box 1 expression in chronic periodontitis tissues, we performed immunohistochemical staining. As seen for gingival crevicular fluid (Fig. 1), most of the inflamed gingival epithelial cells stained positive for high-mobility-group box 1 in the periphery of the nucleus together with some translocation from the nucleus to the cytoplasm in all specimens (Fig. 2A, a,d), whereas staining showed the high-mobility-group box 1 to be localized only in the nuclei of the control cells (Fig. 2A, g,j). Cells were negatively stained with nonspecific IgG (Fig. 2A, b,e,h,k). Recent studies have demonstrated active secretion of high-mobility-group box 1 by macrophages and monocytes during tissue injury (3,8,26). Therefore, we confirmed the origin of the high-mobility-group box 1 by double-immunostaining the same tissue sample with a high-mobility-group box 1 antibody and a macrophage marker antibody (anti-CD68). Only macrophage-like cells showed positive staining for CD68, whereas no positive signals for CD68 were detected in the high-mobility-group box 1-positive gingival epithelial cells (Fig. 2B), indicating that gingival epithelial cells are the source of high-mobility-group box 1 in periodontitis.

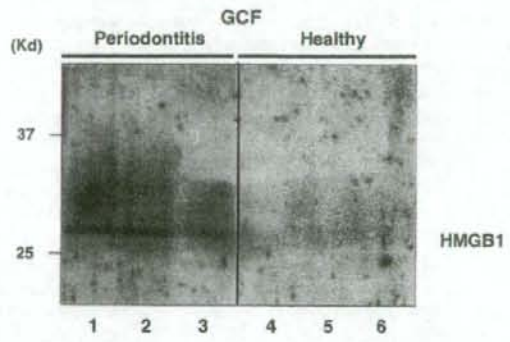

Fig. 1. High-mobility-group box 1 release into gingival crevicular fluid. Western blot analyses with a high-mobility-group box 1 antibody were performed on gingival crevicular fluid samples from three separate patients with periodontitis (lanes 1–3) and from three healthy control subjects (lanes 4–6). High-mobility-group box 1 is present in the gingival crevicular fluid from the periodontitis patients, but absent from that from the control subjects. GCF, gingival crevicular fluid; HMGB1, high-mobility-group box 1.

Tumor necrosis factor receptor 1-dependent high-mobility-group box 1 release into supernatants from rat gingival epithelial cells and Ca9-22 cells

Tumor necrosis factor-α plays a central role in gingival inflammation and is predominantly produced by activated macrophages that invade a lesion following dental plaque or bacteria becoming trapped in a periodontal pocket (27). As described above, we found that high-mobility-group box 1 was localized in both the nucleus and the cytoplasm of epithelial cells in gingival tissues of chronic periodontitis. Thus, we next explored high-mobility-group box 1 release from gingival epithelium stimulated with tumor necrosis factor-α *in vitro*. High-mobility-group box 1 was released constitutively and abundantly into culture medium from both rat gingival epithelial cells and Ca9-22 cells in a dose-dependent (Fig. 3A) and time-dependent (Fig. 3B) manner. No high-mobility-group box 1 was detected in the media from either cell type before stimulation. High-mobility-group box 1 release increased in proportion to the tumor necrosis factor-α concentration until 10 ng/mL and was present at similar levels for samples from both cell types (Fig. 3A). Beyond 20 h, the trend of increasing high-mobility-group box 1 release by tumor necrosis factor-α reached a plateau, probably because of saturation (Fig. 3B).

High-mobility-group box 1 is passively released upon necrotic cell death (6). It was therefore important to ascertain that high-mobility-group box 1 release was from viable rat gingival epithelial cells and Ca9-22 cells, rather than a result of the cytotoxicity of tumor necrosis factor-α. To address this issue, rat gingival epithelial cells and Ca9-22 cells were exposed to various concentrations of tumor necrosis factor-α for up to 24 h, and the cell viabilities were analyzed by the MTT assay. No tumor necrosis factor-α concentration up to 10 ng/mL (i.e. the highest concentration tested in this study) exerted cytotoxic effects on the cells (Fig. 3C), indicating direct dependency of the high-mobility-group

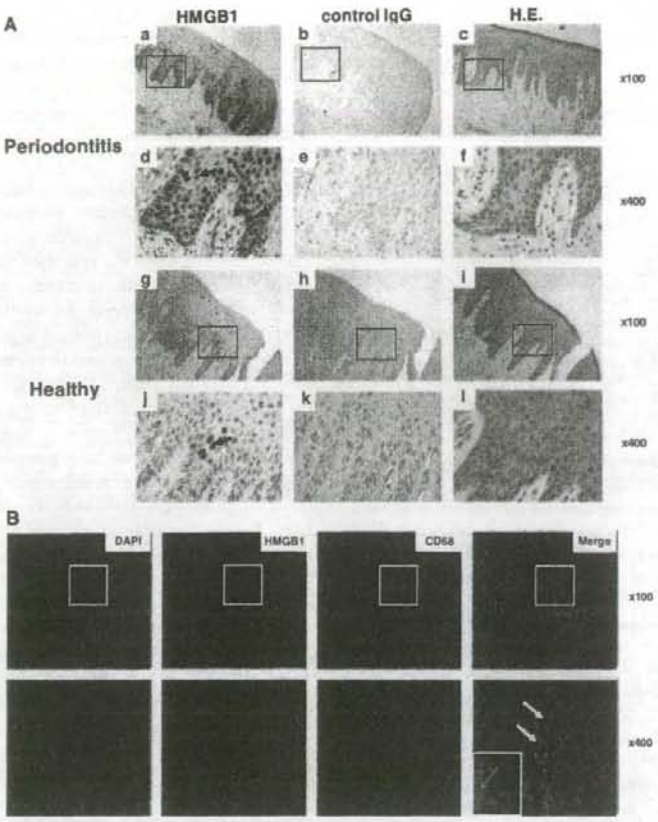

Fig. 2. Cytoplasmic high-mobility-group box 1 expression in inflamed gingival tissues. (A) High-mobility-group box 1 expression in inflamed gingival tissues. The arrow and arrowhead indicate high-mobility-group box 1 positivity in both the nucleus and cytoplasm of gingival epithelial cells, respectively (a and d). Healthy gingival tissues show high-mobility-group box 1 localization in the nucleus (arrow, g and j). Hematoxylin and eosin staining was employed at the same time (c, f, i and l). Magnifications: ×100 (rows 1 and 3) and ×400 (rows 2 and 4). (B) Double immunostaining of high-mobility-group box 1 antibody (green) and a human macrophage marker (CD68; red). High-mobility-group box 1 shuttled to the periphery of the nucleus (yellow arrow). The white arrows indicate CD68-positive staining. Magnifications: ×100 (upper row of panels) and ×400 (lower row of panels). DAPI, 4', 6-diamidino-2-phenylindole; H.E., hematoxylin and eosin; HMGB1, high-mobility-group box 1.

box 1 release from viable gingival epithelial cells upon tumor necrosis factor-α exposure. The similar high-mobility-group box 1 up-regulation patterns between primary cell cultures of rat gingival epithelial cells and the cell line Ca9-22 (Fig. 3A,B) suggest that Ca9-22 cells can serve as a suitable model for further studies on the regulation of high-mobility-group box 1 synthesis.

The biological effects of tumor necrosis factor-α are mediated through its interaction with two distinct receptors, tumor necrosis factor receptor 1 (p55) and tumor necrosis factor receptor (p75), on target cells (28). High-mobility-group box 1 up-regulation is correlated with the extent of chronic diseases, such as rheumatoid arthritis (8). We performed blocking studies using neutralizing antibodies against tumor necrosis factor receptor 1 and tumor necrosis factor receptor 2 overlaid on the cells before stimulation with tumor necrosis factor-α, and detected high-mobility-group box 1 release into the supernatants. These blocking studies revealed inhibition of tumor necrosis factor-α-induced high-mobility-group box 1 release by the tumor necrosis factor receptor 1-neutralizing antibody (Fig. 3D), whereas the tumor necrosis factor receptor 2 neutralizing antibody had no effect (data not shown). Simultaneous incubation with both anti-tumor necrosis factor receptor immunoglobulin showed no cumulative inhibitory effect (data not shown). Taken together, these results indicate that high-mobility-group box 1 release from Ca9-22 cells can be induced through tumor necrosis factor-α/tumor necrosis factor receptor 1 ligation.

P38MAPK-mediated tumor necrosis factor-α-induced high-mobility-group box 1 release

MAPKs are involved in tumor necrosis factor receptor 1-initiated signal transduction in some cells (29,30), resulting in increased high-mobility-group box 1 release (10,31). To clarify the pathway recruited in Ca9-22 cells in response to the persistent presence of tumor necrosis factor-α, we investigated the activation of Jun N-terminal kinase 1/2, p38MAPK and p44/42 by western blot analyses with antibodies that specifically recognize each kinase or its phosphorylated form (Fig. 4A). Phosphorylation of Jun N-terminal kinase 1/2 (Fig. 4A, top panel) and p38MAPK (Fig. 4A, middle panel) was detected within 3.5 min of exposure to tumor necrosis factor-α and sustained until 30 min after exposure. Tumor necrosis factor-α also induced the phosphorylation of p44/42 within 15 min of exposure, followed by a sudden decrease (Fig. 4A, bottom panel). In parallel, our results also revealed specific inhibition of all MAPK isoforms following pre-incubation with their respective inhibitors (Jun N-terminal kinase1/2: SP600125; p38MAPK: SB203580; p44/42: U0126; Fig. 4A, last lanes of each panel).

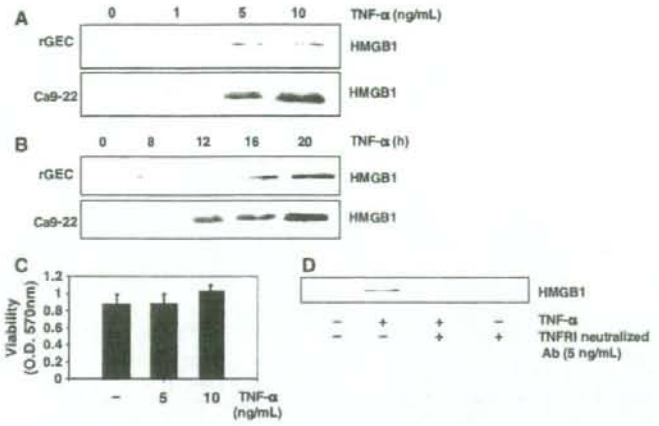

Fig. 3. Tumor necrosis factor receptor 1-dependent high-mobility-group box 1 release into the supernatants of cultured gingival epithelial cells. (A) Rat gingival epithelial cells (upper panel) and Ca9-22 cells (lower panel) were incubated with various concentrations of tumor necrosis factor-α (1, 5 or 10 ng/mL) for 12 h. (B) Rat gingival epithelial cells (upper panel) and Ca9-22 cells (lower panel) were incubated with 5 ng/mL of tumor necrosis factor-α for 0, 8, 12, 16 or 20 h, before aliquots of the supernatants containing equal amounts of protein were separated by sodium dodecyl sulfate-polyacrylamide gel electrophoresis and analyzed by western blotting. (C) Cell viability as a function of tumor necrosis factor-α concentration. Cells were incubated with various concentrations of tumor necrosis factor-α (1–10 ng/mL). Cell viability was measured, after 24 h, by the 3-(4,5-dimethylthiazol-2yl)-2,5-diphenol tetrazolium bromide (MTT) assay, as described in the Material and methods. (D) Inhibition of high-mobility-group box 1 by a tumor necrosis factor receptor 1-neutralizing antibody. Ca9-22 cells were pre-incubated with a tumor necrosis factor receptor 1-neutralizing antibody for 1 h before being stimulated with 5 ng/mL of tumor necrosis factor-α for 12 h. Aliquots of the supernatants containing equal amounts of protein were separated by sodium dodecyl sulfate-polyacrylamide gel electrophoresis and analyzed by western blotting. The results of duplicate experiments are shown. Ab, antibody; HMGB1, high-mobility-group box 1; rGEC, rat gingival epithelial cells; TNF-α, tumor necrosis factor-α; TNFRI, tumor necrosis factor receptor 1.

Next, we endeavored to confirm the specificity of the U0126 inhibitory effects. We showed, in Fig. 4B (top panel), that U0126 selectively ablated the tumor necrosis factor-α-activated phosphorylation of p44/42 (top panel), but did not affect the levels of phospho-p38 or phospho Jun N-terminal kinase 1/2. Interestingly, high-mobility-group box 1 protein was reduced to about 30% ($P < 0.05$) following SB203580 treatment, whereas U0126 and SP600125 had no significant effect (Fig. 4C). These results clearly suggest that the phosphorylation of p38MAPK contributes to more than half of the signaling initiated by tumor necrosis factor-α-elicited high-mobility-group box 1 release.

Discussion

The present study has shown that high-mobility-group box 1 is present in gingival tissues with chronic periodontitis, released from gingival epithelial cells and involved in excessive inflammation regulated by the tumor necrosis factor-α/p38MAPK pathway. These results suggest that continued release of high-mobility-group box 1 over time following stimulation can act, at least in part, as an important amplification signal for progressive periodontal destruction.

In the present study, we found that human gingival crevicular fluid in chronic periodontitis contained high-mobility-group box 1, whereas that from healthy control subjects did not (Fig. 1). In addition, high-mobility-group box 1 was located in the nucleus in healthy tissues, but translocated from the nucleus to the cytoplasm of epithelial cells in the chronic periodontal tissues (Fig. 2A). This finding implies that high-mobility-group box 1 is a highly motile protein that can shuttle to the cytosol via nuclear pores and be released from the cells into the gingival crevice in the inflammatory state. In Fig. 2, macrophages in the connective tissue also expressed high-mobility-group box 1, as reported previously (8,10). Interestingly, high-mobility-group box 1 was strongly detected in gingival epithelial cells. Therefore, we focused on the regulation and expression of high-mobility-group box 1 in gingival epithelial cells. To the best of our knowledge, this is the first report to demonstrate that gingival epithelial cells are the source of high-mobility-group box 1. Immunohistochemical results suggest that translocation of high-mobility-group box 1 in epithelial cells with periodontitis lesions may be affected by stimulation with inflammatory mediators.

Accordingly, we next examined the possibility of bridge formation between tumor necrosis factor-α and high-mobility-group box 1 in stimulated gingival cells, and found a direct dependency of high-mobility-group box 1 extracellular release upon tumor necrosis factor-α exposure. Specifically, tumor necrosis factor-α induced high-mobility-group box 1 release from rat gingival epithelial cells and Ca9-22 cells in a dose- and time-dependent manner. Previous studies have reported delayed kinetics of high-mobility-group box 1 secretion (8–24 h after stimulation), compared with early kinetics, such as tumor necrosis factor-α and interleukin-1, which are secreted within minutes of stimulation with lipopolysaccharide (3,32,33). In keeping with these *in vitro* secretion kinetics, high-mobility-group box 1 was found to increase in serum at 16–32 h after treatment with lipopolysaccharide in an experimental model (3). In the present study, high-mobility-group box 1 release into the supernatants from rat gingival epithelial cells and

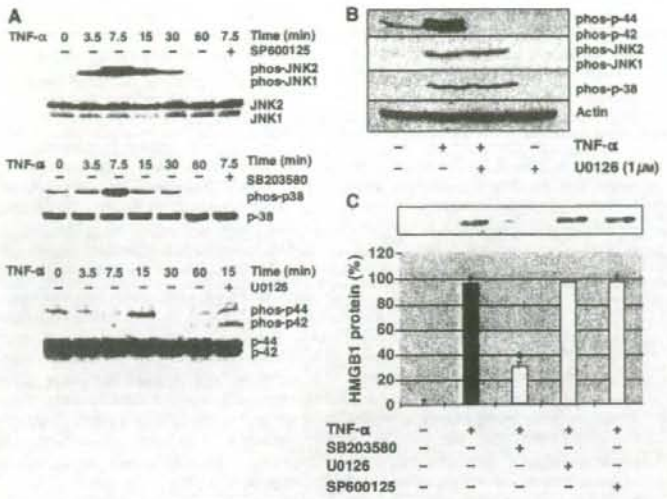

Fig. 4. p38 Mitogen-activated protein kinase (MAPK) phosphorylation in Ca9-22 cells treated with tumor necrosis factor-α, and its contribution to high-mobility-group box 1 release. (A) Cells were incubated with 5 ng/mL of tumor necrosis factor-α for 0–60 min, and the activation of Jun N-terminal kinase 1/2 (top), p38MAPK (middle) and p44/p42 (bottom) was determined by western blot analyses using antibodies that specifically recognize the activated or inactivated forms of these kinases. In the last lanes of panel A, cells were premixed for 1 h with 1 μM SB203580, U0126 or SP600125, and were then incubated in the presence of 5 ng/mL of tumor necrosis factor-α for 7.5 min (top and middle) or 15 min (bottom). (B) Cells were pre-incubated for 1 h with 1 μM U0126 before the addition of 5 ng/mL of tumor necrosis factor-α for 15 min, and then were evaluated by western blot analysis using phospho-p44/p42 (top panel), phospho-Jun N-terminal kinase 1/2 (second panel) and phospho-p38MAPK (third panel) antibodies. (C) Cells were premixed for 1 h with 1 μM SB203580, U0126 or SP600125 and were then incubated in the presence of 5 ng/mL of tumor necrosis factor-α for 12 h. Aliquots of the supernatants containing equal amounts of protein were separated by sodium dodecyl sulfate-polyacrylamide gel electrophoresis and analyzed by western blotting. The high-mobility-group box 1 suppression levels were evaluated using computer-generated images and are shown relative to the highest high-mobility-group box 1 concentration, which was set as 100. $*p < 0.05$, $n = 3$ in each group. The values are presented as means ± standard deviation. JNK, Jun N-terminal kinase; TNF-α, tumor necrosis factor-α.

Ca9-22 cells was only detected after the cells had been exposed to tumor necrosis factor-α for at least 8 h, and the secretion continued for an unusually long period (20 h).

The signaling pathways of MAPKs (p38MAPK, p44/42 and Jun N-terminal kinase) play important roles in inflammatory diseases, such as septic shock, rheumatoid arthritis, atherosclerosis and periodontitis, as well as in other physiological processes (10,34–38). We found that p38MAPK-mediated high-mobility-group box 1 secretion is stimulated by tumor necrosis factor-α, consistent with a previous study showing that lipopoly saccharide-induced high-mobility-group box 1 release is mediated through the p38MAPK signaling pathway (31). However, another recent study reported that high-mobility-group box 1 release occurs independently of p38MAPK (10). This discrepancy may be caused by differences in the cell types and stimulants examined.

In previous studies, tumor necrosis factor-α was reported to induce cytokine release (39,40), and the addition of high-mobility-group box 1 was reported to induce *de novo* cytokine synthesis [e.g. tumor necrosis factor-α, interleukin-1α, interleukin-1β, interleukin-6, interleukin-8, macrophage-inflammatory protein-1α and macrophage-inflammatory protein-1β but not interleukin-10 or interleukin-12 (41)]. In the present study, we demonstrated that high-mobility-group box 1 release was promoted by tumor necrosis factor-α. Therefore, both tumor necrosis factor-α and the endogenous high-mobility-group box 1 may be involved in the up-regulation of cytokine production. Accordingly, cytokine release by tumor necrosis factor-α should be considered to be a result of the involvement of endogenous high-mobility-group box 1. Further studies using neutralizing anti-high-mobility-group box 1 immunoglobulin are needed to confirm this.

Taken together, we have demonstrated that high-mobility-group box 1 release from gingival epithelial cells stimulated by tumor necrosis factor-α may be involved in the progression of periodontitis. Therefore, understanding the mechanisms of high-mobility-group box 1 may lead to novel therapeutic approaches in chronic periodontitis. Further studies are still required to examine the roles of high-mobility-group box 1 in periodontal pathology.

Acknowledgements

This work was supported, in part, by Grants-in-Aid (no. 18390561 and no. 17100007) for Scientific Research from the Ministry of Education, Science and Culture of Japan and Health and Labour Sciences Research Grants from the Ministry of Health, Labour and Welfare.

References

1. Mosevitsky MI, Novitskaya VA, Iogannsen MG, Zabezhinsky MA. Tissue specificity of nucleo-cytoplasmic distribution of HMG1 and HMG2 proteins and their probable functions. *Eur J Biochem* 1989;**185**:303–310.
2. Lu J, Kobayashi R, Brill SJ. Characterization of a high mobility group 1/2 homolog in yeast. *J Biol Chem* 1996;**271**:33678–33685.
3. Wang H, Bloom O, Zhang M *et al.* HMG-1 as a late mediator of endotoxin lethality in mice. *Science* 1999;**285**:248–251.

4. Mullins GE, Sunden-Cullberg J, Johansson AS *et al.* Activation of human umbilical vein endothelial cells leads to relocation and release of high-mobility group box chromosomal protein 1. *Scand J Immunol* 2004;**60**:566–573.
5. Wang H, Vishnubhakat JM, Bloom O *et al.* Proinflammatory cytokines (tumor necrosis factor and interleukin 1) stimulate release of high mobility group protein-1 by pituicytes. *Surgery* 1999;**126**:389–392.
6. Scaffidi P, Misteli T, Bianchi ME. Release of chromatin protein HMGB1 by necrotic cells triggers inflammation. *Nature* 2002;**418**:191–195.
7. Taguchi A, Blood DC, del Toro G *et al.* Blockade of RAGE-amphoterin signalling suppresses tumour growth and metastases. *Nature* 2000;**405**:354–360.
8. Taniguchi N, Kawahara K, Yone K *et al.* High mobility group box chromosomal protein 1 plays a role in the pathogenesis of rheumatoid arthritis as a novel cytokine. *Arthritis Rheum* 2003;**48**:971–981.
9. Park JS, Svetkauskaite D, He Q *et al.* Involvement of toll-like receptors 2 and 4 in cellular activation by high mobility group box 1 protein. *J Biol Chem* 2004;**279**:7370–7377.
10. Kalinina N, Agrotis A, Antropova Y *et al.* Increased expression of the DNA-binding cytokine HMGB1 in human atherosclerotic lesions: role of activated macrophages and cytokines. *Arterioscler Thromb Vasc Biol* 2004;**24**:2320–2325.
11. Dumitriu IE, Baruah P, Manfredi AA, Bianchi ME, Rovere-Querini P. HMGB1: guiding immunity from within. *Trends Immunol* 2005;**26**:381–387.
12. Socransky SS, Haffajee AD, Cugini MA, Smith C, Kent RL Jr. Microbial complexes in subgingival plaque. *J Clin Periodontol* 1998;**25**:134–144.
13. Graves DT, Jiang Y, Genco C. Periodontal disease: bacterial virulence factors, host response and impact on systemic health. *Curr Opin Infect Dis* 2000;**13**:227–232.
14. Verweij CL. Tumour necrosis factor gene polymorphisms as severity markers in rheumatoid arthritis. *Ann Rheum Dis* 1999;**58**:120–126.
15. Graves DT, Cochran D. The contribution of interleukin-1 and tumor necrosis factor to periodontal tissue destruction. *J Periodontol* 2003;**74**:391–401.
16. Stashenko P, Dewhirst FE, Peros WJ, Kent RL, Ago JM. Synergistic interactions between interleukin 1, tumor necrosis factor, and lymphotoxin in bone resorption. *J Immunol* 1987;**138**:1464–1468.
17. Nair SP, Meghji S, Wilson M *et al.* Bacterially induced bone destruction: mechanisms and misconceptions. *Infect Immun* 1996;**64**:2371–2380.
18. Delima AJ, Oates T, Assuma R *et al.* Soluble antagonists to interleukin-1 (IL-1) and tumor necrosis factor (TNF) inhibits loss of tissue attachment in experimental periodontitis. *J Clin Periodontol* 2001; **28**:233–240.
19. Katz J, Bhattacharyya I, Farkhondeh-Kish F *et al.* Expression of the receptor of advanced glycation end products in gingival tissues of type 2 diabetes patients with chronic periodontal disease: a study utilizing immunohistochemistry and RT-PCR. *J Clin Periodontol* 2005;**32**:40–44.
20. Tanaka N, Yonekura H, Yamagishi S *et al.* The receptor for advanced glycation end products is induced by the glycation products themselves and tumor necrosis factor-alpha through nuclear factor-kappa B, and by 17beta-estradiol through Sp-1 in human vascular endothelial cells. *J Biol Chem* 2000;**275**:25781–25790.
21. Nakamura-Minami M, Furuichi Y, Ishikawa K, Mitsuzono-Tofuku Y, Izumi Y. Changes of alpha1-protease inhibitor and secretory leukocyte protease inhibitor levels in gingival crevicular fluid before and after non-surgical periodontal treatment. *Oral Dis* 2003;**9**:249–254.
22. Matsuyama T, Kawai T, Izumi Y, Taubman MA. Expression of major histocompatibility complex class II and CD80 by gingival epithelial cells induces activation of CD4+ T cells in response to bacterial challenge. *Infect Immun* 2005;**73**:1044–1051.
23. Tancharoen S, Sarker KP, Imamura T *et al.* Neuropeptide release from dental pulp cells by RgpB via proteinase-activated receptor-2 signaling. *J Immunol* 2005;**174**:5796–5804.
24. Twentyman PR, Luscombe M. A study of some variables in a tetrazolium dye (MTT) based assay for cell growth and chemosensitivity. *Br J Cancer* 1987; **56**:279–285.
25. Lamster IB. Evaluation of components of gingival crevicular fluid as diagnostic tests. *Ann Periodontol* 1997;**2**:123–137.
26. Abraham E, Arcaroli J, Carmody A, Wang H, Tracey KJ. HMG-1 as a mediator of acute lung inflammation. *J Immunol* 2000;**165**:2950–2954.
27. Rossomando EF, Kennedy JE, Hadjimichael J. Tumour necrosis factor alpha in gingival crevicular fluid as a possible indicator of periodontal disease in humans. *Arch Oral Biol* 1990;**35**:431–434.
28. MacEwan DJ. TNF receptor subtype signalling: differences and cellular consequences. *Cell Signal* 2002;**14**:477–492.
29. Sheng WS, Hu S, Ni HT *et al.* TNF-alpha-induced chemokine production and apoptosis in human neural precursor cells. *J Leukoc Biol* 2005;**78**:1233–1241.
30. Amrani Y, Ammit AJ, Panettieri RA Jr. Tumor necrosis factor receptor (TNFR) 1, but not TNFR2, mediates tumor necrosis factor-alpha-induced interleukin-6 and RANTES in human airway smooth muscle cells: role of p38 and p42/44 mitogen-activated protein kinases. *Mol Pharmacol* 2001;**60**:646–655.
31. Chen G, Li J, Ochani M *et al.* Bacterial endotoxin stimulates macrophages to release HMGB1 partly through CD14- and TNF-dependent mechanisms. *J Leukoc Biol* 2004;**76**:994–1001.
32. Michie HR, Manogue KR, Spriggs DR *et al.* Detection of circulating tumor necrosis factor after endotoxin administration. *N Engl J Med* 1988;**318**:1481–1486.
33. Hesse DG, Tracey KJ, Fong Y *et al.* Cytokine appearance in human endotoxemia and primate bacteremia. *Surg Gynecol Obstet* 1988;**166**:147–153.
34. Duan W, Chan JH, Wong CH, Leung BP, Wong WS. Anti-inflammatory effects of mitogen-activated protein kinase kinase inhibitor U0126 in an asthma mouse model. *J Immunol* 2004;**172**:7053–7059.
35. Han Z, Boyle DL, Chang L *et al.* c-Jun N-terminal kinase is required for metalloproteinase expression and joint destruction in inflammatory arthritis. *J Clin Invest* 2001;**108**:73–81.
36. Nishikawa M, Myoui A, Tomita T *et al.* Prevention of the onset and progression of collagen-induced arthritis in rats by the potent p38 mitogen-activated protein kinase inhibitor FR167653. *Arthritis Rheum* 2003;**48**:2670–2681.
37. Sfakianakis A, Barr CE, Kreutzer D. Mechanisms of *Actinobacillus actinomycetemcomitans*-induced expression of interleukin-8 in gingival epithelial cells. *J Periodontol* 2001;**72**:1413–1419.
38. Brunius G, Domeij H, Gustavsson A, Yucel-Lindberg T. Bradykinin upregulates IL-8 production in human gingival fibroblasts stimulated by interleukin-1beta and tumor necrosis factor alpha. *Regul Pept* 2005;**126**:183–188.
39. Alvaro-Gracia JM, Zvaifler NJ, Brown CB, Kaushansky K, Firestein GS. Cytokines in chronic inflammatory arthritis. VI. Analysis of the synovial cells involved in granulocyte-macrophage colony-stimulating factor production and gene expression in rheumatoid arthritis and its regulation by IL-1 and tumor necrosis factor-alpha. *J Immunol* 1991; **146**:3365–3371.
40. Arend WP, Dayer JM. Inhibition of the production and effects of interleukin-1 and tumor necrosis factor alpha in rheumatoid arthritis. *Arthritis Rheum* 1995;**38**:151–160.
41. Andersson U, Wang H, Palmblad K *et al.* High mobility group 1 protein (HMG-1) stimulates proinflammatory cytokine synthesis in human monocytes. *J Exp Med* 2000;**192**:565–570.

Xenotransplantation 2007: 14: 636–641
Printed in Singapore. All rights reserved
doi: 10.1111/j.1399-3089.2007.00434.x

Brief Communication

XENOTRANSPLANTATION

HMGB1 release in co-cultures of porcine endothelial and human T cells

Kawahara K-i, Setoyama K, Kikuchi K, Biswas KK, Kamimura R, Iwata M, Ito T, Morimoto Y, Hashiguchi T, Takao S, Maruyama I. HMGB1 release in co-cultures of porcine endothelial and human T cells. Xenotransplantation 2007; 14: 636–641. © Blackwell Munksgaard, 2007

Abstract: High mobility group box-1 (HMGB1) protein, primarily from the nucleus, is released into the extracellular milieu either passively by necrotic or damaged cells, or actively by secretion from monocytes/macrophages. Extracellular HMGB1 acts as a potent inflammatory stimulator by promoting cytokine (for example, tumor necrosis factor-α) production, and also has pro-coagulant activity. The signaling pathway initiated by receptor for advanced glycation end-product (RAGE), which is the HMGB1 receptor, also induces complement activation. Recent studies have implicated HMGB1 in acute cardiac allograft rejection, and have identified infiltrating T cells and other damaged cells as its main sources. HMGB1 blockade using the anti-HMGB1 antibody HMGB1 box-A (amino-terminal region) and soluble RAGE rescues mice from acute rejection. We therefore studied the release of HMGB1 in co-cultures of porcine aortic endothelial cells (PAEC) and human leukocytes. Human T cells, but not B cells, monocytes or neutrophils, stimulated significant HMGB1 release in culture with PAEC; this activity required cell–cell contact and was dose-dependent, as determined by Western blotting. The released HMGB1 originated from both cell types, as immunofluorescent microscopy showed that it was present in the cytosol of PAEC in contact with T cells, and had disappeared from the T-cell nuclei. These results demonstrate that direct interactions between PAEC and T cells might be a key factor in triggering HMGB1 release, which suggests that HMGB1 is associated with graft rejection in the early phase.

Ko-ichi Kawahara,[1] Kentaro Setoyama,[2] Kiyoshi Kikuchi,[1] Kamal Krishna Biswas,[1] Ryozo Kamimura,[2] Masahiro Iwata,[3] Takashi Ito,[1] Yoko Morimoto,[4] Teruto Hashiguchi,[1] Sonshin Takao[2] and Ikuro Maruyama[1]

[1]Department of Laboratory and Vascular Medicine Cardiovascular and Respiratory Disorders Advanced Therapeutics, Kagoshima University Graduate School of Medical and Dental Science, Kagoshima, Japan, [2]Frontier Science Research Centre, Kagoshima University, Kagoshima, Japan, [3]Department of Dermatology, Kagoshima University Graduate School of Medical and Dental Science, Kagoshima, Japan, [4]Department of Periodontology, Kagoshima University Graduate School of Medical and Dental Sciences.

Key words: high mobility group box-1 – porcine aortic endothelial cell – T-cell – xenotransplantation

Abbreviations: BSA, bovine serum albumin; CRP, C-reactive protein; DAPI, 4',6-diamidino-2-phenylindole; FBS, fetal bovine serum; FITC, fluorescein isothiocyanate; HAR, hyperacute rejection; HMGB1, high mobility group box-1; HRP, horseradish peroxidase; IFN-g, interferon-g ; IgG, immunoglobulin G; IL, interleukin; LPS, lipopolysaccharide; MTT, 3-(4,5-dimethylthiazol-2-yl)-2,5-diphenyltetrazolium bromide; NIH, National Institutes of Health; PAEC, porcine aortic endothelial cell; PBS, phosphate-buffered saline; PBST, phosphate-buffered saline containing 0.1% Triton-X100; RAGE, receptor for advanced glycation end-product; RT, room temperature; SDS-PAGE, sodium dodecyl sulfate-polyacrylamide gel electrophoresis; TBS, tris-buffered saline; TBST, tris-buffered saline containing 0.02% Tween 20; Th1, T-helper 1; TNF-a, tumor necrosis factor-a; VCAM-1, vascular cell-adhesion protein 1.

Address reprint requests to Ikuro Maruyama, MD, PhD, Department of Laboratory and Vascular Medicine Cardiovascular and Respiratory Disorders Advanced Therapeutics, Kagoshima University Graduate School of Medical and Dental Science, 8-35-1 Sakuragaoka, Kagoshima, 890-8520, Japan (E-mail: rinken@m3.kufm.kagoshima_u.ac.jp)

Received 15 August 2007;
Accepted 5 September 2007

Introduction

Xenotransplantation, especially the transfer of pig organs to humans, has been widely studied as a solution to the shortage of human donor organs. The greatest problem with xenotransplantation is the immunological reaction mounted by the host against non-self grafts. Although the contribution of innate and adaptive immunity to hyperacute rejection (HAR) has been studied extensively for decades, it remains the biggest challenge for xenotransplantation. Recently, the generation of α-1,3-galactosyltransferase knock-out pigs, which lack the major epitope against which natural human antibodies are produced, has provided a source of organs that should eliminate HAR [1–3]. However, as other processes, including vascular rejection and complement activation, remain active, the mechanisms involved in graft rejection require further investigation.

High mobility group box-1 (HMGB1) protein is a promising therapeutic target for the treatment of graft rejection. Blockade of HMGB1 using anti-HMGB1 antibody, HMGB1 box-A (amino-terminal region) and soluble receptor for advanced glycation end-product (RAGE) has been shown to rescue mice from acute organ rejection [4,5]. HMGB1 has pleiotropic effects both inside and outside cells. In the nucleus, HMGB1 promotes the assembly of other nuclear proteins on DNA by bending the molecule [6]. Extracellular HMGB1 released from necrotic or activated cells triggers cell permeability, cell recruitment, cell–cell attachment, cytokine production (tumor necrosis factor-α [TNF-α], interleukin-8, and C-reactive protein), T-cell activation, T-helper 1 (Th1)-cell polarization, dendritic-cell maturation, tissue regeneration and coagulant activation [7–17]. By contrast, signaling from the RAGE, the HMGB1 receptor, activates complement [18]. HMGB1 might therefore play a pivotal role as an enhancer of inflammatory responses in acute rejection, although this has yet to be confirmed.

The current study focused on whether the interactions between porcine aortic endothelial cells (PAEC) and human leukocytes (T cells, B cells, monocytes and neutrophils) triggered HMGB1 release.

Materials and methods

Cell culture

Porcine aortic endothelial cells were purchased from Cell Applications Inc. (San Diego, CA, USA), and were cultured in porcine endothelial cell growth medium (Cell Applications Inc.) supplemented with 100 U/ml penicillin and 100 mg/ml streptomycin. The cells were used at 90% confluence, and the experiments were carried out in RPMI1640 (Sigma-Aldrich, St. Louis, MO, USA) containing 2% fetal bovine serum (FBS; HyClone, Logan, UT, USA).

Isolation of leukocytes

Human leukocytes were harvested from whole blood containing 3.8% (w/v) sodium citrate from healthy volunteers, who had given their informed consent. The cells were isolated by positive selection, as described previously [19]. Briefly, T cells, B cells and monocytes were isolated using Lymphoprep tubes (Axis-Shild, Oslo, Norway), and neutrophils were isolated using Mono-poly resolving medium (Dainippon Sumitomo Pharmaceutical Co. Ltd., Tokyo, Japan). Using a cell isolation kit according to the manufacturer's protocol, $CD3^+$, $CD19^+$, $CD14^+$ and $CD15^+$ cells were isolated by a magnetic cell sorting system (Miltenyi Biotec, Bergisch, Gladbach, Germany). The purity of the cells was >95% as assessed by flow cytometry.

Interactions between human leukocytes and PAEC

Approximately 1.0×10^6 PAEC were seeded into each well of six-well plates. The next day, the PAEC were washed with RPMI1640 medium containing 2% FBS, and then 1 ml RPMI1640 medium was added to each well. The PAEC were incubated with 1.0×10^6 leukocytes (T cells, B cells, monocytes and neutrophils) per well, either together in the well or in a Falcon cell culture insert (Becton Dickinson Labware, Franklin Lakes, NJ, USA). After 3 h, 2 ml samples of the supernatants were collected from the co-cultured cells.

Western blotting

The HMGB1 content of the culture supernatants described above was analyzed by western blotting, as described previously [15,17]. Briefly, each culture supernatant was incubated with 50 ml heparin-Sepharose 6B beads for 4 h. The heparin beads were then washed three times with 10 mM phosphate buffer (pH 7.0), mixed with 50 ml sample buffer (62.5 mM Tris-HCl [pH 6.8], 2% sodium dodecyl sulfate [SDS], 10% glycerol and 0.002% bromophenol blue) and boiled for 5 min. These HMGB1 samples (40 μl) were subjected to 12% SDS–polyacrylamide gel electrophoresis (PAGE), and the separated proteins were then transferred to

a nitrocellulose membrane (Amersham Biosciences, Piscataway, NJ, USA). The membrane was blocked with 5% non-fat dry milk in tris-buffered saline (TBS; pH 7.4) containing 0.02% Tween 20 (TBST) for 1 h at room temperature (RT), and then incubated with 2 μg/ml anti-HMGB1 antibody (Shino-Test, Kanagawa, Japan) in TBST containing 1% non-fat dry milk for 3 h at RT. After washing, the membrane was incubated with horseradish peroxidase (HRP)-conjugated anti-rabbit immunoglobulin G (IgG) polyclonal antibody (Santa Cruz Biotechnology Inc., Santa Cruz, CA, USA) diluted 1 : 3000 in TBST containing 2.5% non-fat dry milk for 1 h at RT. The membrane was washed again, and then the immunoreactive bands were visualized using the ECL detection system (Amersham Biosciences).

Immunofluorescent microscopy

Immunofluorescent microscopy was carried out as described previously [15,16]. Briefly, 5×10^5 PAEC per well were cultured in four-well BioCoat collagen I culture slides (Becton Dickinson Labware) with human T cells (5×10^5 cells/well) for 3 h. As controls, PAEC and T cells were cultured separately in slide chambers. All of the slides were washed with phosphate-buffered saline (PBS), incubated with fluorescein isothiocyanate (FITC)-labeled anti-human CD3 antibody (Becton Dickinson Labware) for 15 min, and then fixed with 250 μl OptiLyse C (Becton Dickinson Labware) containing 0.1% Triton X100 (Sigma-Aldrich). The slides were blocked with 1% bovine serum albumin (BSA) in PBS containing 0.1% Triton-X100 (PBST) for 1 h, incubated with 1 mg/ml rabbit anti-HMGB1 polyclonal antibody for 1 h at RT, and then washed with PBST. The slides were incubated with Alexa Fluor 594-labeled goat anti-rabbit IgG (Invitrogen, Carlsbad, CA, USA) for 1 h, washed with PBST and finally labeled with 4′,6-diamidino-2-phenylindole (DAPI; Nakalai Tesque, Kyoto, Japan) to visualize the cell nuclei. After washing, the slides were examined using an Axioskop microscope (Carl Zeiss, Oberkochen, Germany).

Statistical analysis

The intensity of the protein bands on the western blots was quantified using National Institutes of Health (NIH, Bethesda, MD, USA) Image 1.63 software. The statistical significance of differences in band intensities was determined using the Student's *t*-test and a P-value of 0.05 was taken to be significant.

Results

HMGB1 release in co-cultures of PAEC and T cells, but not other leukocytes

We hypothesized that interactions between donor and recipient cells triggered HMGB1 release. Recent studies have implicated HMGB1 from infiltrating inflammatory cells in graft rejection [4,5]. Therefore, by co-culturing PAEC with leukocytes, we investigated whether cell–cell contact triggered HMGB1 release. Initially, leukocytes, including lymphocytes, monocytes and neutrophils, harvested from whole blood cells containing 0.3% citrate using Mono-poly resolving medium, were added to wells containing PAEC or to Falcon cell

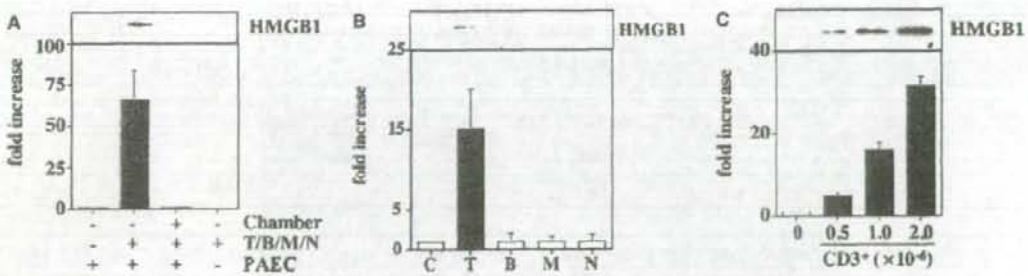

Fig. 1. High mobility group box-1 (HMGB1) release results from cell–cell interactions between porcine aortic endothelial cells (PAEC) and T cells. (A) Western blots showed that HMGB1 release resulted from cell–cell interactions between PAEC and human T cells, but did not occur when the two cell populations were separated by Falcon cell culture inserts. Culture supernatants were collected after 3 h, HMGB1 was extracted with heparin-Sepharose and separated by 12% SDS–PAGE for blotting. HMGB1 bands were detected with anti-HMGB1 antibody. (B) Western blots showed that HMGB1 release was triggered by cell–cell interactions between PAEC and human T cells, but not B cells, monocytes or neutrophils. Different leukocyte populations were purified from whole blood, and 1.0×10^6 cells were cultured with 1.0×10^6 PAEC for 3 h. (C) Quantification of western blots showed that HMGB1 release increased as increasing numbers of T cells were co-cultured with PAEC for 3 h. The protein bands were measured using NIH image 1.63 software.

culture inserts in the wells, and co-cultured for 3 h. As shown in Fig. 1A, there was a 66-fold greater amount of HMGB1 in supernatants in which PAEC and leukocytes had been in direct cell–cell contact compared with the controls, but no significant release of HMGB1 was detected when the cells were separated by Falcon cell culture inserts.

To further investigate these results, we examined which leukocytes triggered HMGB1 release by separating T cells, B cells, monocytes and neutrophils, and incubating the different populations with PAEC for 3 h. As shown in Fig. 1B, T cells triggered a 15-fold increase in HMGB1 release by direct interactions with PAEC, while B cells, monocytes and neutrophils did not. Moreover, as shown in Fig. 1C, incubating increasing numbers of T cells (from 0.5 to 2.0 × 10^6 cells/well) with PAEC induced dose-dependent increases in the levels of HMGB1 release, suggesting that the interactions between PAEC and T cells triggered the HMGB1 release.

HMGB1 release by interactions between PAEC and T cells

We next assessed whether the HMGB1 released into the supernatant originated from the PAEC or the T cells, using immunofluorescent microscopy. PAEC were incubated with or without T cells in four-slide culture chambers for 3 h. As shown in Fig. 2, in co-cultures of PAEC and T cells, HMGB1 was translocated into the cytosol of the PAEC (arrows in Fig. 2) from the nucleus. By contrast, in the T cells, HMGB1 disappeared from the nuclei (arrowheads in Fig. 2). However, T cells and PAEC that were not in direct contact with each other failed to release HMGB1, suggesting that cell–cell interaction is a significant factor in triggering HMGB1 release.

Discussion

We have demonstrated for the first time that cell–cell interactions between PAEC and T cells trigger HMGB1 release, while B cells, monocytes and neutrophils co-cultured with PAEC do not have a similar effect. We have also shown that HMGB1 release increases as the number of T cells in contact with the PAEC increases.

Several lines of evidence suggest that HMGB1 might play a major role in graft rejection. Firstly, the administration of thrombin and HMGB1 together in rats resulted in excessive fibrin deposition, demonstrating pro-coagulant activity [14], and the RAGE signaling pathway, in which HMGB1 is a ligand, activates complement [18], suggesting that HMGB1 might contribute to both vascular events and complement activation in acute rejection. Secondly, treatment of allograft recipients with RAGE, anti-HMGB1 antibody or HMGB1 box-A (amino-terminal region), which specifically block endogenous HMGB1, significantly prolonged the survival of transplanted hearts in murine models [4,5].

Our data also showed that the interactions between PAEC and T cells specifically triggered HMGB1 release in vitro, and that the optimal time for HMGB1 release was 3 h under our conditions (data not shown). We previously reported that the sources of extracellular HMGB1 were activated monocytes/macrophages, vascular smooth-muscle cells and epithelial cell lines [15–17,20]. Other work has shown that endothelial cells induce HMGB1

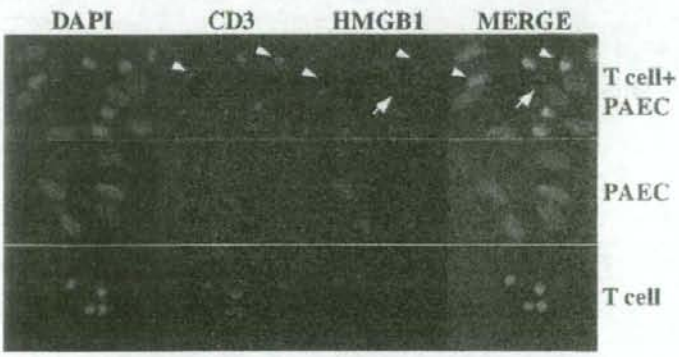

Fig. 2. Cellular localization of high mobility group box-1 (HMGB1) in interacting porcine aortic endothelial cells (PAEC) and T cells. PAEC and T cells were incubated together in slide chambers for 3 h. As controls, PAEC and T cells were also cultured separately. The slides were fixed and incubated with FITC-labeled anti-CD3 and anti-HMGB1 antibodies. After washing, the slides were incubated with Alexa Fluor 594-labeled goat anti-rabbit IgG. Nuclei were labeled with DAPI. Original magnification was ×400. Arrowheads indicate the disappearance of HMGB1 from the nuclei of T cells incubated with PAEC. Arrows indicate the translocation-of HMGB1 in PAEC, resulting from interactions with T cells.

release [21], suggesting that it can be induced by all cell types. Interestingly, we used immunofluorescent microscopy to demonstrate that HMGB1 release resulted from interactive cell–cell stimulation, and originated form both PAEC and T cells. However, monocytes, neutrophils and B cells did not trigger HMGB1 release under our conditions, suggesting that the period of time for which these cells were co-cultured with PAEC might not have been sufficient for HMGB1 release.

Moreover, HMGB1 was released from cells activated by TNF-α, interferon-γ and lipopolysaccharide or necrotic cells, suggesting that this activity might have been triggered by cytokines in our study. However, previous reports have implied that cytokine induction by cell–cell interactions occurs after >24 h culture [22], and not within 3 h. Although it is possible that HMGB1 release induced by cell–cell interactions (especially by CD8 T cells) might be caused by cell death, the death of T cells and PAEC was not induced by cell–cell interactions for 3 h in a 3-(4,5-dimethylthiazol-2-yl)-2,5-diphenyltetrazolium bromide assay (data not shown). Furthermore, the mechanism of HMGB1 release has been suggested to involve interactions between vascular cell-adhesion protein 1 (VCAM-1) or E-selectin of endothelial cells and molecules of T cells. Resting and activated T cells induced VCAM-1 and E-selectin expression by endothelial cells, but not other cell types, after 2 to 4 h [22]. Therefore, interactions between T cells co-cultured with PAEC specifically triggered the release of HMGB1, but not other factors, such as cytokine induction and cell death induced by CD8 T cells.

Although recent studies have suggested that damaged cells and infiltrating T cells are the source of HMGB1 in tissue grafts [4,5], HMGB1 release might have been initiated when the recipients were challenged with donor tissue, further suggesting that the source of HMGB1 in vivo might be the blood vessels. Moreover, HMGB1 release might not be an entirely immunological effect, but might occur merely as a result of cell–cell interactions. We believe that this finding suggests a new therapeutic approach to the control of HMGB1 release. We plan to further investigate the mechanism of HMGB1 release using in vivo graft rejection studies, in order to identify the molecules on PAEC and T cells that are involved.

To the best of our knowledge, this is the first report to demonstrate that the interactions of PAEC and T cells directly trigger HMGB1 release. The HMGB1 released from these cells has the potential to amplify graft rejection and, in addition, could contribute to the accumulation of inflammatory cells in transplanted organs, thereby further promoting the development of graft rejection.

Acknowledgments

We thank Nobue Uto, Tomoka Nagasato and Hisayo Sameshima for their excellent technical assistance. This study was supported by research grants from the Ministry of Education, Culture, Sports, Science, and Technology of Japan, by Grant-in-Aid 17100007 (S.T.) and 18791341 (T.I.), and by a Health and Labor Sciences Research Grant from the Ministry of Health, Labor and Welfare (I.M.).

References

1. Kaiser J. Xenotransplantation. Cloned pigs may help overcome rejection. Science 2002; 295: 25–27.
2. Lai L, Kolber-simonds D, Park KW et al. Production of alpha-1,3-galactosyltransferase knockout pigs by nuclear transfer cloning. Science 2002; 295: 1089–1092.
3. Phelps CJ, Koike C, Vaught TD. Production of alpha 1,3-galactosyltransferase-deficient pigs. Science 2003; 299: 411–414.
4. Huang Y, Yin H, Han J et al. Extracellular HMGB1 functions as an innate immune-mediator implicated in murine cardiac allograft acute rejection. Am J Transplant 2007; 7: 799–808.
5. Moser B, Szablocs MJ, Ankersmit HJ et al. Blockade of RAGE suppresses alloimmune reactions in vitro and delays allograft rejection in murine heart transplantation. Am J Transplant 2007; 7: 293–302.
6. Agresti A, Bianchi ME. HMGB proteins and gene expression. Curr Opin Genet Dev 2003; 13: 170–178.
7. Andersson U, Wang H, Palmblad K et al. High mobility group 1 protein (HMG-1) stimulates proinflammatory cytokine synthesis in human monocytes. J Exp Med 2000; 192: 565–570.
8. Scaffidi P, Misteli T, Bianchi ME. Release of chromatin protein HMGB1 by necrotic cells triggers inflammation. Nature 2002; 418: 191–195.
9. Rovere-querini P, Capobianco A, Scaffidi P et al. HMGB1 is an endogenous immune adjuvant released by necrotic cells. EMBO Rep 2004; 5: 825–830.
10. Palumbo R, Sampaolesi M, De Marchis F et al. Extracellular HMGB1, a signal of tissue damage, induces mesoangioblast migration and proliferation. J Cell Biol 2004; 164: 441–449.
11. Yang D, Chen Q, Yang H et al. High mobility group box-1 protein induces the migration and activation of human dendritic cells and acts as an alarmin. J Leukoc Biol 2007; 81: 59–66.
12. Dumitriu IE, Baruah P, Valentinis B et al. Release of high mobility group box 1 by dendritic cells controls T cell activation via the receptor for advanced glycation end products. J Immunol 2005; 174: 7506–7515.
13. Messmer D, Yang H, Telusma G. High mobility group box protein 1: an endogenous signal for dendritic cell maturation and Th1 polarization. J Immunol 2004; 173: 307–313.
14. Ito T, Kawahara K, Nakamura T et al. High-mobility group box 1 protein promotes development of

microvascular thrombosis in rats. J Thromb Haemost 2007; 5: 109–116.
15. Morimoto Y, Kawahara K, Tancharoen S et al. Tumor necrosis factor-a stimulates gingival epithelial cells to actively release high mobility group box 1. J Periodontal Res (in press).
16. Taniguchi N, Kawahara K, Yone K et al. High mobility group box chromosomal protein 1 plays a role in the pathogenesis of rheumatoid arthritis as a novel cytokine. Arthritis & Rheumatism 2003; 48: 971–981.
17. Inoue K, Kawahara K, Kamal KB et al. HMGB1 expression by activated vascular smooth muscle cells in advanced human atherosclerosis plaques. Cardiovasc Pathol 2007; 16: 136–143.
18. Johnson LV, Leffner WP, Rivest AJ et al. The Alzheimer's a beta-peptide is deposited at sites of complement activation in pathologic deposits associated with aging and age-related macular degeneration. Proc Natl Acad Sci U S A 2002; 99: 11830–11835.
19. Dirk RL, Frank D, Uwe W et al. Immunoglobulin A1 protease, an exoenzyme of pathogenic *Neisseriae*, is a potent inducer of proinflammatory cytokines. J Exp Med 1999; 190: 1049–1058.
20. Kawahara K, Kamal KB, Unoshima M et al. CRP induces high mobility group box-1 protein release through a p38MAPK in the macrophage cell line RAW264.7 cells. Cardiovasc Pathol (in press).
21. Mullins GE, Sunden-cullberg J, Johansson AS et al. Activation of human umbilical vein endothelial cells leads to relocation and release of high-mobility group box chromosomal protein 1. Scand J Immunol 2004; 60: 566–573.
22. Yarwood H, Mason JC, Mahiouz D, Sugars K, Haskard DO. Resting and activated T cells induce expression of E-selectin and VCAM-1 by vascular endothelial cells through a contact-dependent but CD40 ligand-independent mechanism. J Leukoc Biol 2000; 68: 233–242.

Molecular Psychiatry (2007) 12, 976–983

www.nature.com/mp

LETTERS TO THE EDITOR

High mobility group box 1 and refeeding-resistance in anorexia nervosa

Molecular Psychiatry (2007) **12**, 976–977;
doi:10.1038/sj.mp.4002050

Anorexia nervosa (AN) is a serious disorder affecting adolescents and young adults, and decreases quality of life over long period.[1] Successful weight restoration is an important prognostic factor for disease outcome;[1] however, the underlying mechanism of refeeding-resistance (RR), a core psychopathology relevant to 'ambivalent' eating behaviors, remains unclear in this disorder.[2–4]

High mobility group box 1 (HMGB1), a ubiquitous DNA binding protein,[5] plays various extracellular roles as a proinflammatory cytokine, an immune adjuvant, a repair factor for injured tissues and a mediator of anorexia.[6–8] We therefore investigated whether serum HMGB1 levels are associated with acute conditions, refeeding progress or RR in patients with AN.

Eleven female in-patients admitted to Kagoshima University Hospital (age: 23.2±7.8 years; duration of illness: 3.9±4.2 years), who met the DSM-IV criteria for restricting type AN, were consecutively enrolled between January and December 2006. Eleven control participants (age: 23.0±2.2 years; body mass index (BMI): 19.8±1.8 kg/m^2; fasting blood glucose (FBS): 4.9±0.4 mmol/l; serum aspartate aminotransferase (AST): 16.8±2.9 IU/l) were recruited from the local community. Inclusion criteria are described elsewhere.[2,3] The Institutional Committee of Kagoshima University approved the protocol, and written informed consent was obtained from all participants.

During the first hospital week (observation (OB) period), no therapeutic intervention was applied.[2,3,9] On day 7, baseline assessment was made, including body weight (BW), mean values of daily energy intake (EI) and proinflammatory cytokines using high-sensitivity assay such as tumor necrosis factor (TNF)-α, interleukin (IL)-1β (R&D Systems, Minneapolis, MN, USA for both) and IL-6 (Fujirebio Inc., Tokyo, Japan). Serum HMGB1 assay via ELISA was performed (Shino-test Corporation, Kanagawa, Japan).[8]

Thereafter, all patients started the same 12-week treatment program consisting of nutritional rehabilitation and cognitive behavior therapy.[2,3,9] Total daily EI started at 1000 kcal and increased by 200 kcal/week. After completely eating served meals for 1 week, patients were allowed to start the next EI stage. After 1600 kcal/day, weight gain $\geq$0.5 kg/week was required.[2,3,9] If the patient failed for two consecutive weeks owing to fear of obesity (RR period), a second assessment was performed on day 14 of that period. Changes between baseline and the second assessment were determined for serum HMGB1 (delta HMGB1), daily EI (delta EI) and BW (delta BW). We also recorded BW changes during the week before the second assessment (delta BW-RR). Between-group comparisons were performed by Student's *t*-test or one-factor analysis of variance followed by Bonferroni correction using Stat View 5.0.1 (SAS Institute Inc., Cary, NC, USA). Results were expressed as mean±s.d. Significance was set at $P<0.05$.

All patients experienced the RR period (mean time to this period: 9.7±2.2 weeks). AN patients during the OB and RR periods showed significantly lower BMI (13.6±1.8 and 14.4±1.8 kg/m^2, respectively) and FBS values (4.1±0.3 and 4.3±0.2 mmol/l, respectively) than controls ($P<0.0001$ for both). AN patients during the RR period differed from those during the OB period in daily EI (1827±155 vs 1163±233 kcal, $P<0.0001$) and serum AST (23.8±5.2 vs 53.3±45.6 IU/l, $P<0.05$). No significant group effects were detected in cytokines. AN patients during the RR period showed significantly higher HMGB1 values than those during the OB period or controls ($P=0.002$; Figure 1). Delta HMGB1 was positively correlated with delta EI ($r=0.73$; $P=0.01$) and delta BW ($r=0.80$; $P=0.003$) and negatively correlated with delta BW-RR ($r=-0.61$; $P=0.04$).

This study suggests that serum HMGB1 levels may be related to not only refeeding progress (that is, delta BW and delta EI) but also RR (that is, delta BW-RR). Together with these variables, serum HMGB1 levels may form an RR loop in AN patients.

Elucidation of the underlying mechanism of HMGB1 release remains limited. HMGB1 is released passively by necrotic or damaged cells and actively by monocyte/macrophages via proinflammatory cytokines.[5–7] Normalization of malnutritional abnormalities (for example, serum AST) during the RR period may not support the earlier pathway, and our cytokine results may not support the latter pathway. However, recent studies on AN have yielded inconsistent results, with either increased or unchanged serum levels of IL-1β, IL-6 and TNF-α;[10] thus, further studies with a larger sample size are needed to investigate the relationship between serum HMGB1 and cytokine levels in anorexics. Delta HMGB1 values related to refeeding progress suggests that nutritional factors may play an important role in HMGB1 release in anorexics.

The small sample size and lack of examination of central HMGB1 activities may limit this study. HMGB1-induced anorexia is mainly mediated by intracerebral effects;[7] thus, further studies on these

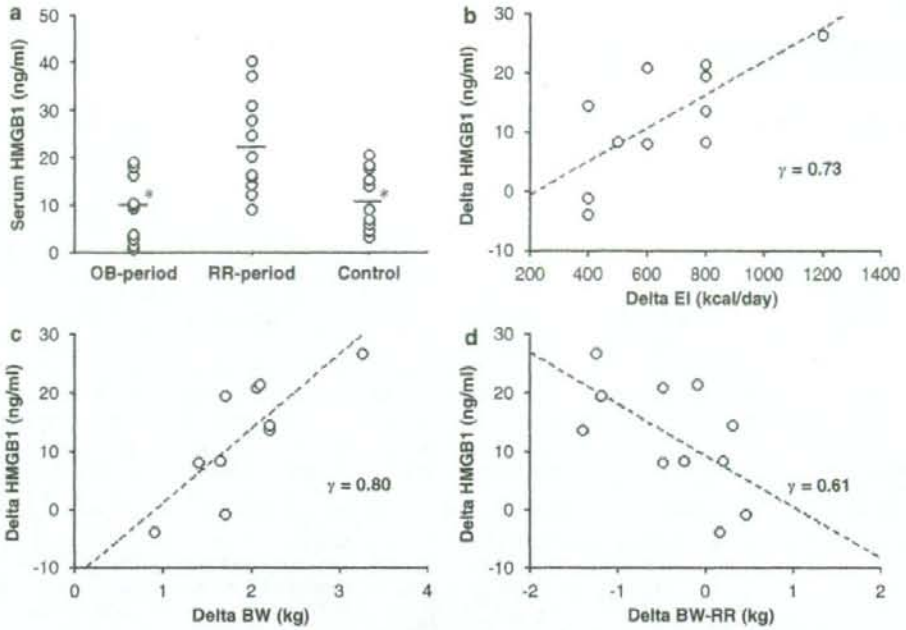

Figure 1 (**a**) Serum high mobility group box 1 (HMGB1) concentrations in anorexics at baseline assessment during the observation period (OB period), anorexics at the second assessment during the refeeding-resistant period (RR period) and controls. Bars indicate mean values. $^*P<0.005$ vs the RR period. (**b**) Correlation between changes in serum HMGB1 concentrations (delta HMGB1) and daily energy intake (delta EI) between baseline and the second assessment. (**c**) Correlation between delta HMGB1 and changes in body weight (BW) between baseline and the second assessment (delta BW). (**d**) Correlation between delta HMGB1 and changes in BW during the week before the second assessment (delta BW-RR).

issues are needed in anorexics. Nonetheless, our findings indicate a close relationship between serum HMGB1, refeeding progress and RR that warrants future investigations as a potential therapeutic target in AN.

D Yasuhara[1], T Hashiguchi[2], K Kawahara[2], T Nakahara[1], T Harada[1], H Taguchi[1], S Yamada[3], I Maruyama[2] and A Inui[1]

[1]Department of Behavioral Medicine, Graduate School of Medical and Dental Sciences, Kagoshima University, Kagoshima, Japan; [2]Department of Laboratory and Vascular Medicine, Graduate School of Medical and Dental Sciences, Kagoshima University, Kagoshima, Japan and [3]Central Institute, Shino-Test Corporation, Sagamihara, Kanagawa, Japan

E-mail: yasuhara@m3.kufm.kagoshima-u.ac.jp

References

1 Steinhausen HC. *Am J Psychiatry* 2002; **159**: 1284–1294.
2 Yasuhara D, Naruo T, Nagai N, Muranaga T, Nakahara T, Tanaka M *et al. Psychosom Med* 2005; **67**: 669–676.
3 Yasuhara D, Naruo T, Nagai N, Tanaka M, Muranaga T, Nozoe S. *Am J Clin Nutr* 2003; **77**: 292–299.
4 Inui A. *Mol Psychiatry* 2001; **6**: 620–624.
5 Bustin M. *Mol Cell Biol* 1999; **19**: 5237–5246.
6 Wang H, Bloom O, Zhang M, Vishnubhakat JM, Ombrellino M, Che J *et al. Science* 1999; **285**: 248–251.
7 Agnello D, Wang H, Yang H, Tracey KJ, Ghezzi P. *Cytokine* 2002; **18**: 231–236.
8 Yamada S, Maruyama I. *Clin Chim Acta* 2007; **375**: 36–42.
9 Yasuhara D, Nakahara T, Harada T, Inui A. *Am J Psychiatry* 2007; **164**: 528–529.
10 Corcos M, Guilbaud O, Paterniti S, Moussa M, Chambry J, Chaouat G *et al. Psychoneuroendocrinology* 2003; **28**: 229–249.

Is ASMT a susceptibility gene for autism spectrum disorders? A replication study in European populations

Molecular Psychiatry (2007) **12**, 977–979;
doi:10.1038/sj.mp.4002069

Several studies have indicated that melatonin, a pineal gland hormone synthesized from serotonin,

INTERNAL MEDICINE

CASE REPORT

Two Cases of Acute Exacerbation of Interstitial Pneumonia Treated with Polymyxin B-immobilized Fiber Column Hemoperfusion Treatment

Satoshi Noma[1], Wataru Matsuyama[1], Hideo Mitsuyama[1], Takayuki Suetsugu[1], Yoshimizu Koreeda[1], Keiko Mizuno[1], Ikkou Higashimoto[1], Yasuyuki Kakihana[2], Teruto Hashiguchi[3], Ikuro Maruyama[3], Mitsuhiro Osame[1] and Kimiyoshi Arimura[1]

Abstract

The effect of polymixin B-immobilized fiber column (PMX) hemoperfusion treatment for acute exacerbation of interstitial pneumonia (IP) has been reported. Here, we report 2 cases of acute exacerbation of IP successfully treated with PMX hemoperfusion. One is a 55-year-old woman who was diagnosed as microscopic polyangiitis (MPA) with IP. The other is a 58-year-old man, diagnosed as having idiopathic pulmonary fibrosis. Both cases were treated with PMX hemoperfusion and other therapies. One died on day 44 and the other is still alive. The PMX hemoperfusion treatment decreased the serum levels of several cytokines and activated neutrophil percentage in bronchoalveolar lavage fluid.

Key words: bronchoalveolar lavage fluid cells, CD18+/CD11c, high mobility group box-1 (HMGB-1)

(DOI: 10.2169/internalmedicine.46.0117)

Introduction

Acute exacerbation of idiopathic pulmonary fibrosis (IPF) is a well-recognized concept (1-3) and that of other IPs, in particular those related to collagen vascular diseases have been also reported (4, 5). However, effective treatments are not well-established and mortality of these patients has been reported to be high during the short course (3, 6, 7). Recent reports have suggested that the use of polymixin B-immobilized fiber column (PMX) hemoperfusion treatment may be effective in patients with acute lung injury (ALI)/acute respiratory distress syndrome (ARDS) and acute exacerbation of idiopathic pulmonary fibrosis(IPF) (8-11). Here, we report two cases of acute exacerbation of IP treated with PMX hemoperfusion treatment. We also show the flow-cytometry results of bronchial lavage fluid (BALF) cells and change of serum cytokine levels before and after PMX hemoperfusion.

Case Report

Case 1

A 55-year-old woman was admitted to our hospital in June 2006 because of dyspnea and cough. One year before admission, she was diagnosed as having microscopic polyangiitis with interstitial pneumonia because renal biopsy showed crescentic necrotizing glomerulonephritis and her serum myeloperoxidase antineutrophil cytoplasmic autoantibody (MPO-ANCA) by enzyme-linked immunosorbent assay (ELISA) was very high (1,937 U/ml, normal range, <9). The chest X-ray and chest high-resolution computed tomography (HRCT) scans showed reticular shadows, ground glass opacities and peripheral subpleural thickening. Her pulmonary symptoms and renal malfunction was improved via the treatment with prednisolone and cyclophosphamide. Three days before admission she developed dyspnea on ef-

[1] Division of Respiratory Medicine, Respiratory and Stress Care Center, Kagoshima University Hospital, Kagoshima, [2] Division of Intensive Care Medicine, Kagoshima University Hospital, Kagoshima and [3] Department of Laboratory and Vascular Medicine Cardiovascular and Respiratory Disorders Advanced Therapeutics, Kagoshima University Graduate School of Medical and Dental Science, Kagoshima

Received for publication February 22, 2007; Accepted for publication May 21, 2007

Correspondence to Dr. Wataru Matsuyama, vega@xa2.so-net.ne.jp

DOI: 10.2169/internalmedicine.46.0117

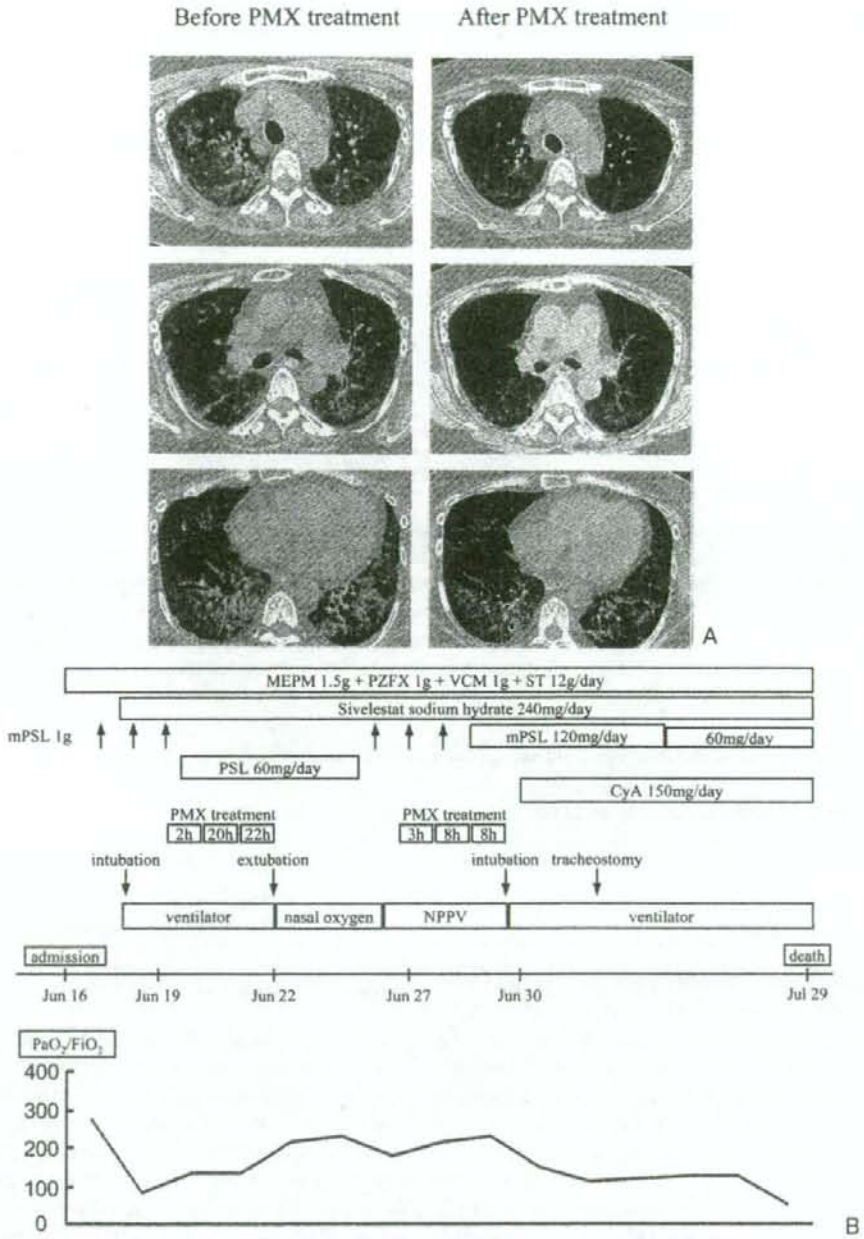

Figure 1. A: Chest HRCT before and after the PMX hemoperfusion treatment of Case 1. Chest HRCT showed improvement of the ground-glass opacity. B: Clinical course of Case 1.

fort and cough. Her symptoms became worse and she was admitted to our hospital. Laboratory findings on admission were as follows: white blood cell count (WBC) 9,700 mm^3; lactate dehydrogenase (LDH) 543 IU/L; C-reactive protein (CRP) 7.43 mg/dl; KL-6 3,373 U/mL. Endotoxin and β-D glucan concentrations were under the detectable limits. MPO-ANCA was 22.0 U/ml. Arterial blood gas analysis under room air showed hypoxia and hypocarbia (pH 7.512, $PaCO_2$ 33.3 mmHg, PaO_2 57.2 mmHg). The chest HRCT scans showed diffuse bilateral ground glass opacities (Fig. 1A). The BALF anlaysis showed an increase in neutrophils with no obvious evidence of infectious disease (Table 1). Her clinical course is shown in Fig. 1B. She was treated with steroid pulse therapy (1 g of methylpredonisolone per day for 3 days), Sivelestat sodium hydrate, and antibiotics. However, the respiratory failure progressed and mechanical ventilation was applied on day 3 after admission. On day 4 we started PMX hemoperfusion treatment

DOI: 10.2169/internalmedicine.46.0117

Table 1. BALF Finding

	Before PMX	After PMX
Case 1		
Total cell count (/μl)	6.41×10^5	1.57×10^5
Macrophage (%)	43	76
Lymphocyte (%)	16	11
Neutrophil (%)	41	12
Eosinophil (%)	1	1
CD4/8	0.89	1.02
CD18+/CD11c+ (%)	34.3	11.2
CXCR2+ (%)	18.2	9.1
CCR2+(%)	18.4	9.3
CD3+/CD25+ (%)	21.8	22.1
CXCR3+ (%)	9.2	9.1
Bacteria	(-)	(-)
PJ-PCR	(-)	(-)
Case 2		
Total cell count (/μl)	0.9×10^5	0.53×10^5
Macrophage (%)	64	44
Lymphocyte (%)	16	17
Neutrophil (%)	16	36
Eosinophil (%)	3	3
CD4/8	2.6	1.7
CD18+/CD11c+ (%)	13.1	9.2
CXCR2+ (%)	9.2	4.1
CCR2+ (%)	13.3	6.3
CD3+/CD25+ (%)	14.1	15.6
CXCR3+ (%)	7.2	7.4
Bacteria	(-)	(-)
PJ-PCR	(-)	(-)

PJ: Pneumocystis jiroveci

(Toraymixin 20R, Toray Medical Co., Tokyo, Japan, a flow rate of 80 ml/min). Nafamostat mesilate (Torii Pharma Co., Tokyo, Japan) was used as an anticoagulant during the PMX treatment. We performed PMX hemoperfusion treatment 3 times (2 hours, 22 hours and 20 hours). After treatment, the PaO_2/FiO_2 (P/F) ratio improved from 64.2 to 229.4, and she was successfully weaned from mechanical ventilation. Chest HRCT showed improvement of the ground-glass opacity (Fig. 1A). The laboratory findings at this point were as follows: lactate dehydrogenase (LDH) 243 IU/L; C-reactive protein (CRP) 0.43 mg/dl; KL-6 2,139 U/mL. Endotoxin and β-D glucan concentrations were under the detectable limits. MPO-ANCA was 7.3 U/ml. BALF after treatment showed decreased total cell counts and neutrophil percentage. Twelve days after the remission, she again developed respiratory failure and we applied mechanical ventilation. The respiratory failure progressed despite the therapy including PMX hemoperfusion treatment and she died because of respiratory failure 44 days after admission (41 days after the first PMX hemoperfusion treatment. An autopsy was performed, which showed diffuse alveolar damage with hyaline membranes and partial organization. Acute bronchopneumonia was found in the right lower lobe.

Case 2

A 58-year-old man was admitted to our hospital because of dyspnea in December 2006. Three years before admission, health examination showed an abnormal chest shadow, but he did not go to the hospital. Eight months before admission, he came to our hospital due to dyspnea on effort. His chest HRCT revealed reticular opacities, honeycombing and traction bronchiectasis with basal and peripheral predominance. There was no evidence of vascular collagen disease, hypersensitivity pneumonitis, pneumoconiosis, sarcoidosis, or vasculitis. He was diagnosed as having IPF clinically according to the criteria of American Thoracic Society/European Respiratory Society (ATS/ERS) international consensus statement (12). His mother had also suffered from interstitial pneumonia and died because of respiratory failure. Five days before admission, he developed dyspnea on effort (Hugh-Jones dyspnea criteria grade II) and cough. The symptoms became worse (Hugh-Jones dyspnea criteria grade IV) and he was admitted to our hospital. Laboratory findings on admission were as follows: WBC 7,700 mm^3; LDH 348 IU/L; CRP 8.32 mg/dl; KL-6 1,548 U/mL. Endotoxin and β-D glucan concentrations were under the detectable limits. Arterial blood gas analysis under room air showed hypoxia (pH 7.425, PCO_2 38.5 mmHg, PO_2 36.1 mmHg). Chest HRCT showed diffuse bilateral ground glass opacities predominantly in lower lobe (Fig. 2A). BALF examination showed an increase of neutrophil percentage with no evidence of infection. His clinical course is shown in Fig. 2B. We started antibiotics, steroid pulse therapy (1 g of methylprednisolone per day for 3 days), cyclophosphamide pulse therapy (500 mg of cyclophosphamide per day), and antibiotic therapy. On day 2 after admission, we started PMX he-

DOI: 10.2169/internalmedicine.46.0117

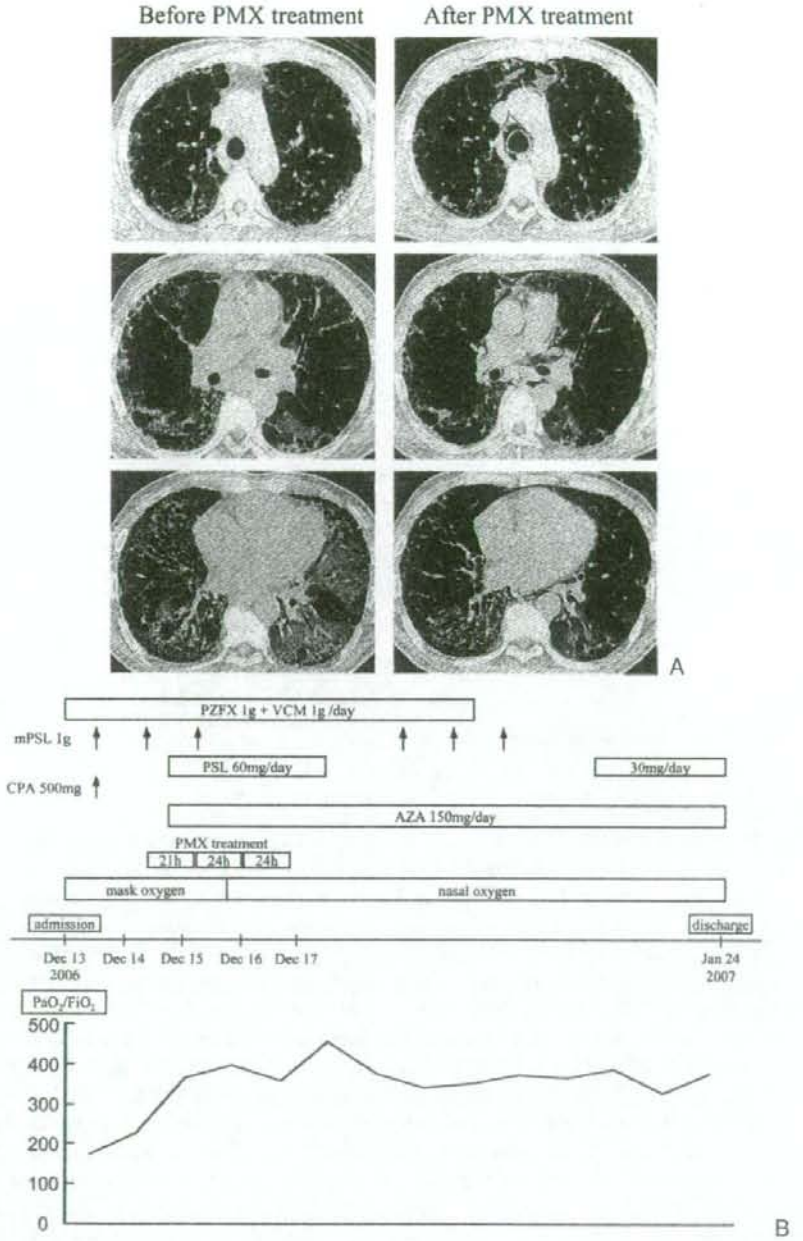

Figure 2. A: Chest HRCT before and after the PMX hemoperfusion treatment of Case 2. Chest HRCT showed improvement of the ground-glass opacity. B: Clinical course of Case 2.

moperfusion treatment (Toraymixin 20R, Toray Medical Co., Tokyo, Japan, at a flow rate of 80 ml/min). Nafamostat mesilate (Torii Pharma Co., Tokyo, Japan) was used as an anticoagulant during the PMX hemoperfusion treatment. We performed PMX hemoperfusion treatment 3 times (20 hours, 24 hours and 24 hours). After PMX hemoperfusion treatment, P/F ratio improved from 225.0 to 395.6. Chest HRCT showed improvement of the ground-glass opacity (Fig. 2A). The laboratory findings at this point were as follows: LDH 221 IU/L; CRP 0.32 mg/dl; KL-6 748 U/mL; endotoxin and β-D glucan were under detectable concentration. BALF examination after PMX hemoperfusion treatment showed decreased total cell counts and an increase of neutrophil percentage. Prednisolone (30 mg/day) and azathioprine (150 mg/day) was administered orally as maintenance therapy. His symptoms improved and he was discharged 44 days af-

DOI: 10.2169/internalmedicine.46.0117

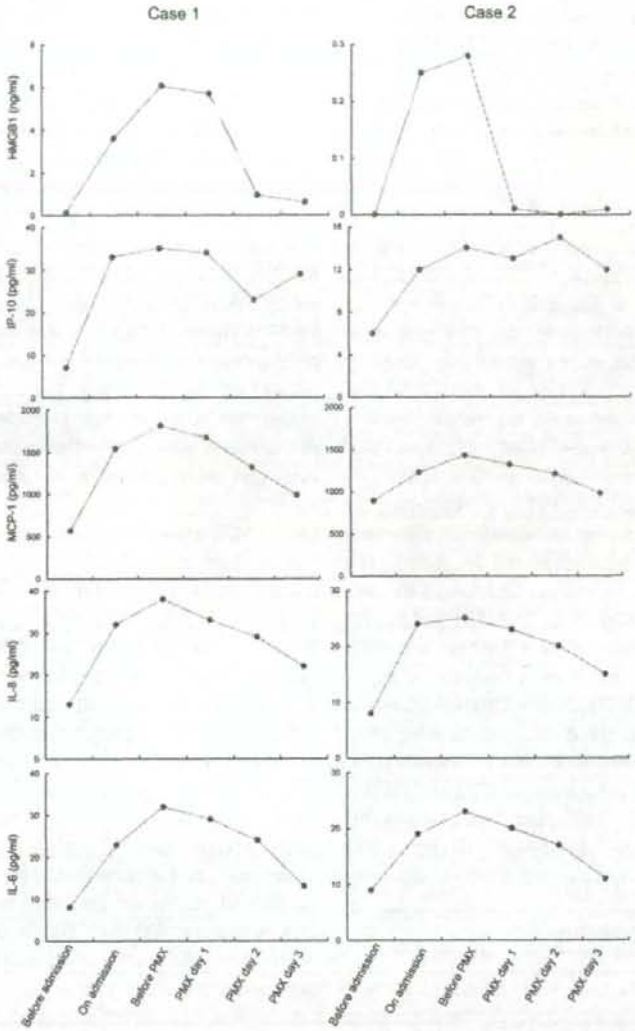

Figure 3. Cytokine changes in sera of our cases during the PMX hemoperfusion treatment. The serum HMGB1 level was undetectable before admission, increased on admission, and decreased remarkably on day 2 after the start of PMX hemoperfusion treatment in both cases. The serum level of IP-10 did not show remarkable change during the PMX hemoperfusion treatment. The serum level of MCP-1, IL-8, and IL-6 decreased on day 3 after the start of PMX hemoperfusion treatment, but was higher than before admission in both cases.

ter admission.

Criteria for the PMX hemoperfusion treatment on acute exacerbation of interstitial pneumonia

As a policy of our department, we administrate PMX hemoperfusion to the patients who fulfill the following criteria: 1) acute exacerbation of interstitial pneumonia; 2) no obvious evidence of infectious disease; 3) P/F ratio does not increase above 300 (criteria for acute lung injury (13)) within 24 hours despite the start of standard treatments for acute exacerbation of interstitial pneumonia.

Measurement of serum cytokine level

We measured interleukin-6 (IL-6), IL-8, monocyte chemoattractant protein-1 (MCP-1) and interferon inducible protein of 10 kDa (IP-10) levels in sera of our patients using a commercial enzyme-linked immunosorbent assay (ELISA) kit (sIL-2R: R&D Systems, Minneapolis, MN). ELISA for high mobility group box 1 (HMGB1) in the sera was performed with the use of monoclonal antibodies to HMGB1 and with standardization to a curve of recombinant human HMGB1 as described previously (14). As shown in Fig. 3, The serum HMGB1 level was undetectable before admission, increased on admission, and decreased remarkably on day 2 after the

DOI: 10.2169/internalmedicine.46.0117

start of PMX hemoperfusion treatment in both cases. The serum level of IP-10 did not show a remarkable change during the PMX hemoperfusion treatment. The serum levels of MCP-1, IL-8, and IL-6 decreased on day 3 after the start of PMX hemoperfusion treatment, but were higher than before admission in both cases.

Flow cytometry analysis of BALF cells

The expression of BALF cell surface CD3, CD18, CD11c, CD25 (interleukin-2 receptor), CXCR2 (receptor of IL-8), CXCR3 (receptor for IP-10) and CCR2 (receptor of MCP-1) (15) was evaluated by flow-cytometry analysis. One hundred thousand BALF cells were suspended in 50 μl of cold PBS containing 0.1% sodium azide, 10 ng/ml BSA and 20 μg/ml of human IgG, incubated for 10 minutes on ice, and with mouse monoclonal anti-CXCR2, CD18, CCR2, CXCR3 or CD25 (PharMingen, SanDiego, CA, USA) IgG antibody and FITC-conjugated anti-CD3 or PE-conjugated CD11c antibody (PharMingen) for an additional 15 minutes on ice. Cells were washed with PBS, and incubated with FITC or PE-conjugated goat anti-mouse IgG for 15 minutes on ice. At the end of the incubation, 7AAD (PharMingen) was added to each tube. The cells were washed with PBS, and subsequently analyzed by flow cytometry using a FACScan (Becton Dickinson). Dead cells, determined by the incorporation of 7AAD, were gated out. Results were processed using the CellQuest software (Becton Dickson).

As shown in Table 1, the percentage of CD18+/CD11c+, CCR2+, and/CXCR2+BALF cell decreased remarkably while CD3+/CD25+ and CXCR3+ BALF cell percentage did not show remarkable change.

Discussion

Acute exacerbations of IPs have been described to have high mortality during short course (3, 6, 7). Recent reports have suggested that PMX hemoperfusion treatment may be effective in patients with ALI/ARDS and acute exacerbation of IPF (8, 9, 11). PMX hemoperfusion treatment can reduce the mortality of ARDS (11) and reduce serum level of metalloproteinase (MMP)-9 tissue inhibitor of MMP (TIMP)-1 (9). Also, PMX hemoperfusion treatment can improve the survival rate of sepsis with renal failure (16) and oxygenation of sepsis patients (17). In particular, Seo et al reported that four of six patients of acute exacerbations of IPF were successfully weaned from mechanical ventilation and survived more than 30 days after the initial PMX hemoperfusion treatment, suggesting the clinical effect of PMX hemoperfusion treatment (10). The present cases also survived more than 30 days, however, the outcome of our two cases was totally different (case 1 died while case 2 is still alive on April 25, 2007). We think this difference might have been due to the following reasons: 1) The difference of timing of PMX hemoperfusion administration [Early administration of PMX hemoperfusion treatment can eliminate humoral mediators and improves pulmonary oxygenation.]. (8); 2) The presence of infection in case 1 (Case 1 showed bronchopneumonia at autopsy). However, it is difficult to determine the true reason for this difference. Detection of the true reason of this difference might provide an important insight to clarify the mechanism of PMX treatment in acute exacerbation of interstitial pneumonia.

The detailed mechanism by which PMX hemoperfusion treatment improves oxygenation has not been fully elucidated. In the present cases, we showed a decrease of IL-8, MCP-1, IL-6, and HMGB1 level in the sera, however, the serum IP-10 level did not change remarkably during the PMX treatment. IL-8, a chemokine that can activate neutrophils through CXCR2 (15), is elevated in IPF and indicates disease activity (18) and is associated with the pathogenesis of MPO-ANCA vasculitis (19). MCP-1, a chemokine that can attract a variety of inflammatory cells including monocytes and neutrophils (15), is a marker of ANCA-associated vasculitis (20) and is involved in the pathogenesis of IPF (21). PMX hemoperfusion treatment can reduce the serum level of IL-6 and HMGB1 (22). IL-6 is an important inflammatory mediator (23). HMGB-1 has recently been proposed as one of the late mediators of sepsis or lipopolysaccharide (LPS) endotoxin lethality (24). Abraham et al demonstrated that the intratracheal administration of recombinant HMGB-1 is a distal mediator of acute inflammatory lung injury (25). Ueno et al suggested that the overexpression of extracellular HMGB-1 plays a key role in the pathogenesis of ALI (26). The modification of these cytokines might be associated with the effect of PMX hemoperfusion treatment on acute exacerbation of interstitial pneumonia.

In the present cases, CD18+/CD11c+ and CXCR2+ BALF cell percentage decreased after the PMX hemoperfusion treatment. CD18+/CD11c+ is a marker of activated neutrophils (27), and CXCR2 is a receptor of IL-8 (15). In our report, we found that a decrease in cytokine is associated with activation of neutrophils. This change might contribute to the decrease of CD18+CD11c positive cells. However, the reason for the increase in neutrophil % after the PMX treatment in case 2 is still unclear. Ambrosini et al reported that in acute exacerbations of IPF, marked neutrophilia was detected in BALF (3). Neutrophils cause damage to the pulmonary vascular endothelium by releasing oxygen radicals, proteinases, leukotrienes, and other proinflammatory molecules such as platelet-activating factor, thus impairing the barrier function of the pulmonary capillaries and leading to the onset of ALI or ARDS (28, 29). In our cases, CCR2+ BALF cell percentage decreased after the PMX hemoperfusion treatment. MCP-1-CCR2 axis contributes to the neutrophil recruitment in lung via alveolar macrophages in lung inflammation (30). In the present cases, CD3+/CD25+ BALF cell percentage and CXCR3 (receptor for of IP-10 (15)) positive cell percentage did not show remarkable change. CD3+/CD25+ cells are activated T lymphocytes (31), and IP-10 is a chemokine that can recruit activated T lymphocytes (32). These results may suggest the relation between the effect of PMX hemoperfusion treatment and acti-